Electronic Supporting Information

Hydroxyl-mediated ethanol selectivity of CO_2 hydrogenation

Chengsheng Yang[1], Rentao Mu[1], Guishuo Wang, Jimin Song, Hao Tian, Zhi-Jian Zhao, and Jinlong Gong*

Key Laboratory for Green Chemical Technology of Ministry of Education, School of Chemical Engineering and Technology, Tianjin University; Collaborative Innovation Center of Chemical Science and Engineering, Tianjin 300072, China;

[1]These authors contributed equally to this work.

*Corresponding author: jlgong@tju.edu.cn

Contents

S1. Characterization details

1.1 Characterization methods

Powder X-ray diffraction (XRD) patterns were performed with 2θ values between 20° and 90° using a Bruker-D8 diffractometer (λ = 1.54056 Å). X-ray photoelectron spectroscopy (XPS) measurements were taken on a PHI 1600 ESCA instrument (PE Company) equipped with an Al Kα X-ray radiation source (hv = 1486.6 eV). Before measurements, all the samples were dried at 50 ℃ for 6 h. The binding energies were calibrated using the C 1s peak at 284.6 eV as a reference.

The morphology of catalysts was characterized by transmission electron microscopy (TEM; FEI Tecnai G2 F20, 200 kV). The TEM was additional equipped with high-resolution electron energy-loss spectroscopy (EELS) for elemental analysis. Annular dark field scanning TEM (ADF-STEM) and energy dispersive X-ray (EDX) mapping were operated with an Oxford X-Max 80 SDD EDX detector at 200 kV. To investigate the molar ratio of different elements, the catalysts, 10 mg each, were dissolved in a perchloric/nitric acid mixture. The concentrations of Rh, Fe and Li in the leached solutions were measured by the inductively coupled plasma optical emission spectroscopy (ICP-OES; Varian 720-ES).

H_2 temperature-programmed reduction (H_2-TPR) and CO temperature-programmed desorption (CO-TPD) were performed on a Micromeritics AutoChem II 2920 apparatus equipped with HIDEN QIC-20 mass spectrometer (MS). For H_2-TPR experiment, 100 mg sample was pretreated at 300 ℃ for 1 h under flowing Ar to remove water and other contamination. After cooling to 50 ℃, 10 vol% H_2/Ar was introduced for the reduction and the temperature was increased from 50 ℃ to 800 ℃ with the ramp rate of 10 ℃/min. The signal was recorded online by thermal conductivity detector (TCD). For CO-TPD experiment, 100 mg sample was pre-reduced at 400 ℃ for 1 h under 10 vol% H_2/Ar. When the temperature was cooled by liquid N_2 and kept stable at -70 ℃, pure CO was introduced for 0.5 h. Subsequently, the purging was carried out by Ar for 1 h. Then the temperature was increased from -70 ℃ to 500 ℃ with the ramp rate of 10 ℃/min. The gas component in the effluent was monitored and recorded online by MS, and the signals for *m/e* of 44, 28 and 18 were monitored.

The Rh on the particle surface was studied by employing the CO chemisorption method. For each test, 200 mg sample was pre-reduced with 10 vol% H_2/Ar at 400 ℃ for 1 h, then cooled to 50 ℃. Subsequently, CO was admitted to the sample by injection pulses of 10 vol% CO/He (0.5082 mL) until the consumption peaks became stable. It can be assumed that the adsorption stoichiometry factor of Rh/CO = 1.[1] The V_{CO} is the active loop volume of CO adsorbed on Rh (mL), *SF* is the stoichiometry factor.

A Micromeritics Tristar 3000 analyzer was used to obtain the textual properties of catalysts by N_2 adsorption-desorption at 77 K. Prior to the tests, all samples were degassed at 300 ℃ for 6 h. The specific surface areas were calculated from the isotherms using the Brunauer-Emmett-Teller (BET) method, and the pore distribution and the cumulative volumes of pores (V_{pore}) were obtained by the Barret-Joyner-Halenda (BJH) method from the desorption branches of the N_2 isotherms.

The Diffuse Reflectance Infrared Fourier Transform Spectroscopy (DRIFTS) was used to record vibrational spectra of molecules adsorbed on the different catalysts. *In situ* DRIFTS experiments were performed on a Thermo Scientific Nicolet IS50 spectrometer, equipped with a Harrick Scientific DRIFTS cell and a mercury-cadmium-telluride (MCT) detector cooled by liquid N_2. About 100 mg finely ground sample was packed in the ceramic crucible of the *in situ* chamber. All the samples were pretreated at 400 ℃ under a H_2 flow (20 mL/min) for 1 h and cooled to the desired temperature to obtain a background spectrum, and the spectra for each measurement was then collected by subtracting the background spectrum. The spectra under reaction conditions were recorded with a

resolution of 4 cm^{-1}. As for the Fourier Transform Infrared (FTIR) spectrum to characterize the surface hydroxyl, 1 mg of sample was mixed in an agate mortar with ~300 mg of potassium bromide (KBr) followed by a thorough drying in a vacuum oven at 200℃. Before mixing, the KBr powder was dried at 500℃ overnight to get rid of water. The mixture was then pressed into a pellet for 5 min using a force of 5 tons, and transparent pellets were obtained. All the pellets were dried in vacuum oven at 120℃ for 3 hours to get rid of water before FTIR tests. We use the pure KBr pellet (~300 mg) as the background and integrate peak area of associative hydroxyl stretching vibrations at 3450 cm^{-1} to represent the amount of the hydroxyl. Furthermore, the peak area of hydroxyl groups normalized by BET surface area (S_{BET}) of catalysts was applied to represent the density of surface hydroxyls.

1.2 Reactivity test

CO_2 conversion, C-containing gas products selectivity, ethanol yield, turnover frequency (TOF) were calculated as follow[2-4]:

$$X_{CO2}(\%) = \frac{F_{CO2,in} - F_{CO2,out}}{F_{CO2,in}} \times 100$$

$$S_i(\%) = \frac{\%\mathrm{i} \times \mathrm{n}}{\sum((\%\mathrm{i}) \times \mathrm{n})} \times 100$$

$$\text{Ethanol yield}(\%) = X_{CO2}(\%) \times S_{ethanol}(\%) \times 100$$

$$TOF\ of\ ethanol = \frac{F_{CO2,in} \times X_{CO2} \times 60 \times S_{ethanol}}{V_{CO} \times SF}(h^{-1})$$

$$TOF\ of\ CH_4 = \frac{F_{CO2,in} \times X_{CO2} \times 60 \times S_{CH4}}{V_{CO} \times SF}(h^{-1})$$

Where *i* represents the carbon containing species in the products, including CH_4, CO, C_nH_m, CH_3OH and C_2H_5OH, and *n* is the number of carbon atoms in the carbon containing species. TOF of CH_4 or ethanol was calculated as moles of CH_4 or ethanol formed on per mole of surface Rh obtained from the CO chemisorption. TOF of CO_2 was calculated as moles of CO_2 converted on per mole of surface Rh. The Data for the catalytic activity were collected when the reaction reached stable conditions, and the repeated tests have been also carried out to confirm the reproducibility of the results. Besides, carbon balances closed to within ±8% for the data.

S2. Supporting tables and figures

2.1 Supporting tables

Table S1. Physicochemical properties of different catalysts.

Catalyst	W_{Rh}[a] /wt%	S_{BET}[b] /m^2 g_{cat}^{-1}	V_{pore}[b] /cm^3 g_{cat}^{-1}
RhFeLi/ TiO_2 NRs-400℃	2.5	22.5	0.08
RhFeLi/ TiO_2 NRs-500℃	2.4	23.6	0.08
RhFeLi/ TiO_2 NRs-600℃	2.5	21.8	0.07
RhFeLi/ TiO_2 Com	2.4	18.2	0.06
RhFeLi/ TiO_2 NRs-CO	2.4	23.1	0.08

a. ICP-AES.
b. N_2 adsorption.

Table S2. Catalytic properties of different catalysts.

Catalyst	d_{Rh}[a] /nm	Active loop volume (CO, cm^3/g STP)	Ethanol yield /%	TOF of CH_4 /h^{-1}	TOF of ethanol /h^{-1}
RhFeLi/TiO_2 NRs-400℃	2.5	0.50	3.1	0.58	0.11
RhFeLi/TiO_2 NRs-500℃	2.3	0.69	5.1	0.21	0.12
RhFeLi/TiO_2 NRs-600℃	2.8	0.42	0.9	0.02	0.04
RhFeLi/TiO_2 Com	4.0	0.09	0.6	0.20	0.08
RhFeLi/TiO_2 NRs-CO	2.7	0.67	0.1	0.01	0.00
RhFeLi/SiO_2	7.1	0.06	0.4	0.09	0.08

a. Diameter of Rh nanoparticles determined by the statistical results of TEM images.

Table S3. Compositions of different catalysts.

Catalyst	Rh:Fe (XPS)	Rh:Fe (ICP-AES)	Rh/wt% (ICP-AES)	Fe/wt% (ICP-AES)
RhFeLi/TiO_2 NRs	58:42	48:52	2.4	1.4
RhFeLi/TiO_2 Com	29:71	50:50	2.4	1.3

Table S4. Binding energies of Rh 3d and Fe 2p, and molar ratio of Rh:Fe for different RhFeLi/TiO_2 catalysts.

Catalyst	RhFeLi/TiO_2 NRs-400℃	RhFeLi/TiO_2 NRs-500℃	RhFeLi/TiO_2 NRs-600℃	RhFeLi/TiO_2 NRs-CO	RhFeLi/TiO_2 Com
Rh $3d_{5/2}$	307.1 eV	307.2 eV	307.1 eV	307.2 eV	306.8 eV
Fe $2p_{3/2}$	710.8 eV	711.0 eV	710.9 eV	711.0 eV	711.3 eV
Rh:Fe (Atomic ratio)	59:41	58:42	56:44	48:52	29:71

Table S5. DRIFTS peak assignments of the surface species for the CO_2 hydrogenation reaction.

Species	Peaks/cm^{-1}	Assignment
Formate	1585-1610	ν_{as}(OCO)
	1361-1370	ν_s(OCO)
	2880-2886	ν(CH)
	1379-1383	δ(CH)
	2970-2977	δ(CH)+ν_{as}(OCO)
	2731-2738	δ(CH)+ν_s(OCO)
Carbonate	1520, 1300-1400	CO_3^{2-}
Methoxy	2931-2935,2821-2825	$\nu(CH_3)$
	1045-1049	$\nu(OCH_3)$
Methyl	1450-1470	δ(C-H)

Table S6. CO_2 conversion and product distribution of CO_2 hydrogenation over different catalysts.[a]

Catalyst	Conversion/%	Selectivity/%				
		CO	CH_4	CH_3OH	C_2H_5OH	Other oxygenates[b]
RhFeLi/TiO_2 NRs-300℃	22.0	5.4	84.7	1.9	7.5	0.5
RhFeLi/TiO_2 NRs-400℃	21.4	5.1	79.5	0.6	14.6	0.2
RhFeLi/TiO_2 NRs-500℃	15.7	12.5	53.9	2.2	31.3	0.1
RhFeLi/TiO_2 NRs-600℃	6.6	77.2	6.7	3.2	12.6	0.3
RhFeLi/TiO_2 Com	4.5	43.9	36.8	3.3	15.7	0.3
RhFeLi/TiO_2 NRs-CO	4.7	81.4	9.6	7.1	1.2	0.7

a. Reaction conditions: 300 mg catalyst, P = 30 atm, T = 250℃, GHSV= 6000 h^{-1}, $CO_2/H_2/N_2$ = 1/3/1.

b. Other oxygenates are mainly C_{2+} oxygenates.

2.2 Supporting figures

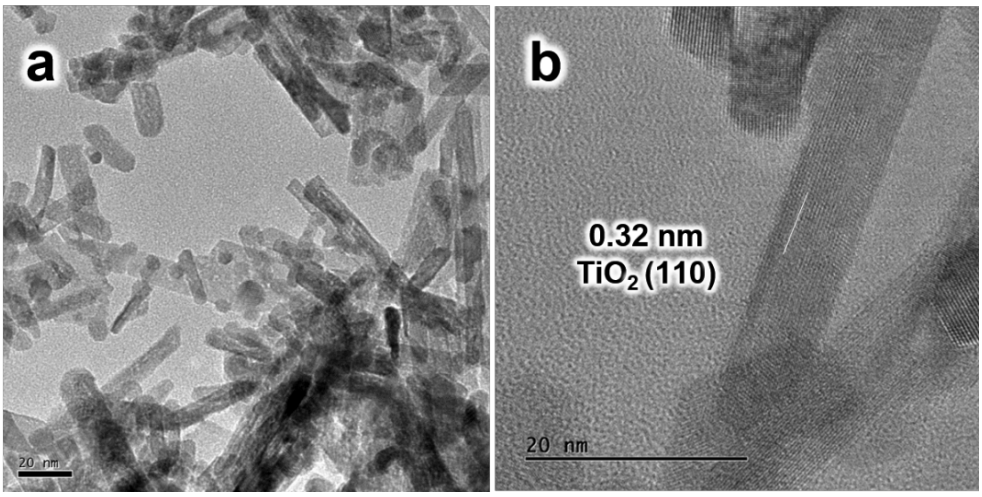

Fig. S1. (a) TEM and (b) HRTEM of TiO_2 NRs. The scale bar represents 20 nm.

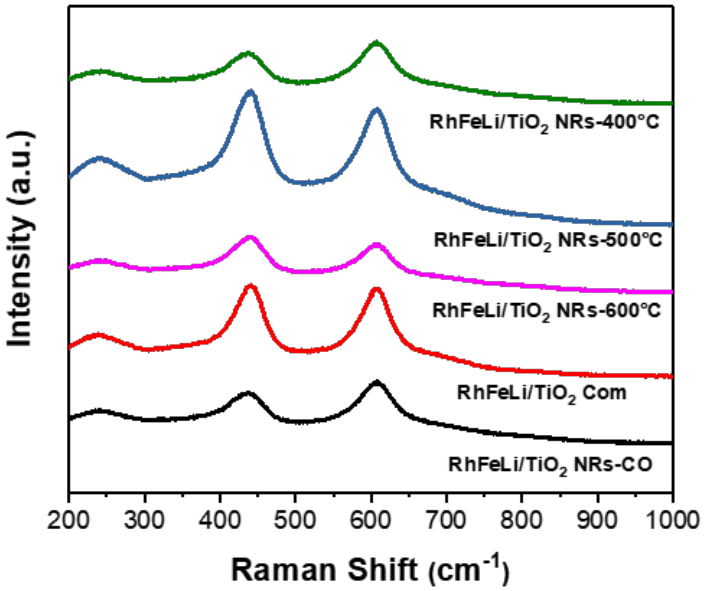

Fig. S2. Raman spectrum ($\lambda_{excitation}$ = 532 nm) of 2.5 wt% RhFeLi supported on different TiO_2 after reaction. The supports include TiO_2 NRs-400℃, TiO_2 NRs-500℃, TiO_2 NRs-600℃, TiO_2 NRs-CO and TiO_2 Com. Raman spectra were recorded under ambient conditions using a 532 nm Ar ion laser beam.

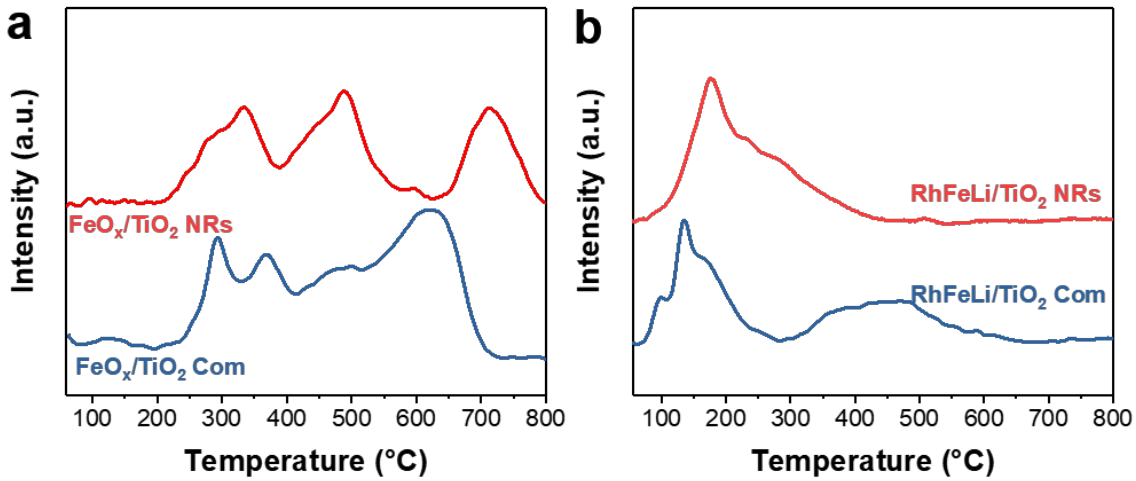

Fig. S3. (a) H_2-TPR profile of 1 wt% FeO_x/TiO_2 NRs and 1 wt% FeO_x/TiO_2 Com. (b) H_2-TPR profile of 2.5 wt% $RhFeLi/TiO_2$ NRs and 2.5 wt% $RhFeLi/TiO_2$ Com.

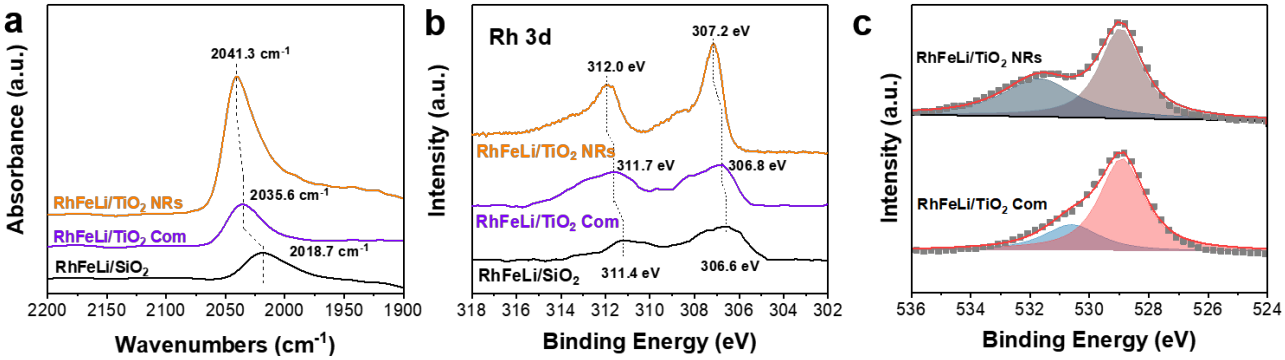

Fig. S4. (a) FTIR spectra over 2.5 wt% RhFeLi/TiO_2 NRs, 2.5 wt% RhFeLi/TiO_2 Com and 2.5 wt% RhFeLi/SiO_2 after CO adsorption at 250℃. (b) XPS spectra of Rh 3d obtained from 2.5 wt% RhFeLi/TiO_2 NRs, 2.5 wt% RhFeLi/TiO_2 Com and 2.5 wt% RhFeLi/SiO_2. (c) XPS spectra of O 1s obtained from 2.5 wt% RhFeLi/TiO_2 NRs and 2.5 wt% RhFeLi/TiO_2 Com. All the data were collected from the catalysts after H_2-reduction.

Note: The O 1s spectrum of RhFeLi/TiO_2 displays two peaks at 529.0 and 531.5 eV (Fig. S4c), which can be attributed to lattice oxygen and hydroxyl groups, respectively.[5-6]

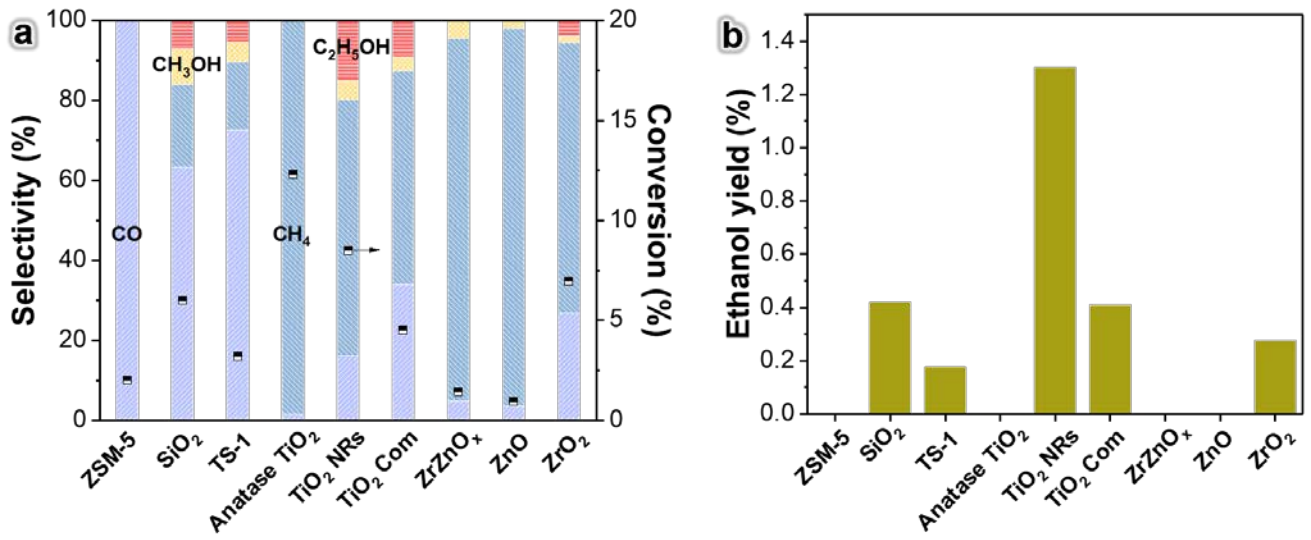

Fig. S5. (a) The comparison of CO_2 conversion (Black symbol) and product distribution (Column) obtained over 1 wt% RhFeLi (Rh:Fe:Li =1:1:1) supported on different supports. (b) The comparison of ethanol yield obtained over 1 wt% RhFeLi (Rh:Fe:Li =1:1:1) supported on different supports. Reaction conditions: P = 30 atm, T = 250 ℃, GHSV = 6000 h^{-1}, $CO_2/H_2/N_2$ = 1/3/1.

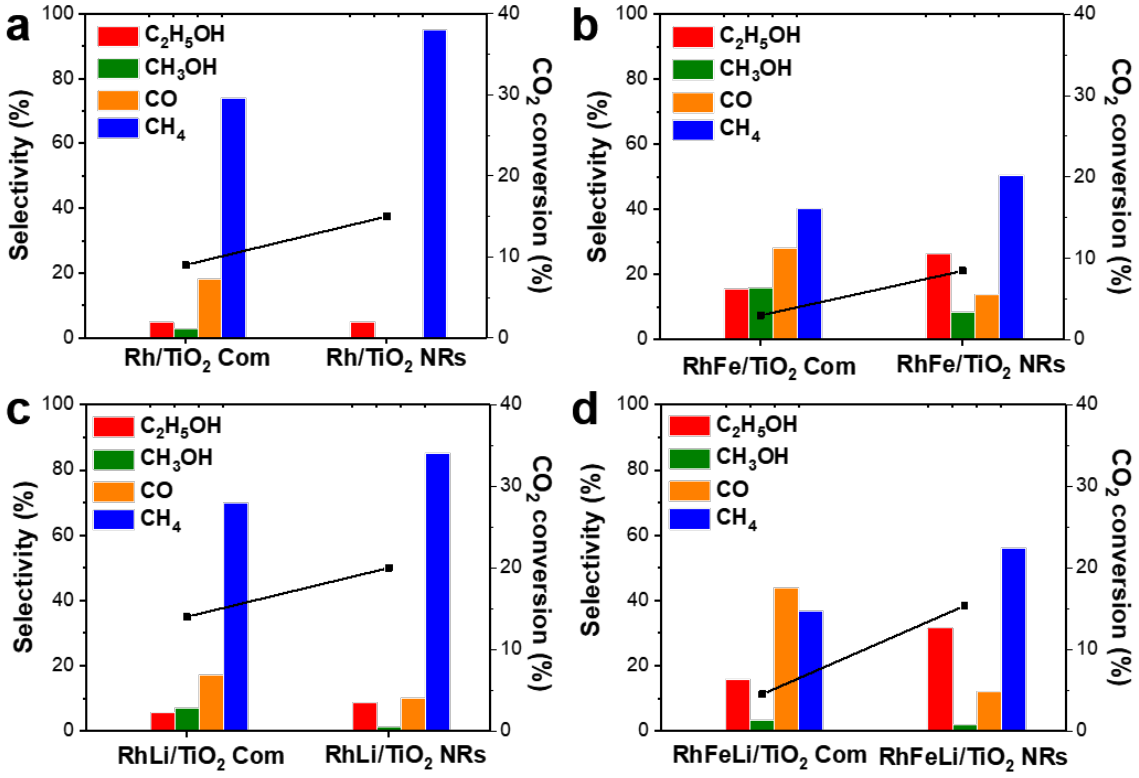

Fig. S6. The CO_2 conversion (Black) and product distribution obtained from 2.5 wt% Rh/TiO_2 NRs and Com (a), 2.5 wt% $RhFe/TiO_2$ NRs and Com (Rh:Fe=1:1) (b), 2.5 wt% $RhLi/TiO_2$ NRs and Com (Rh:Li=1:1) (c), 2.5 wt% $RhFeLi/TiO_2$ NRs and Com (Rh:Fe:Li=1:1:1) (d). Reaction conditions: P = 30 atm, T = 250℃, GHSV = 6000 h^{-1}, $CO_2/H_2/N_2$ = 1/3/1.

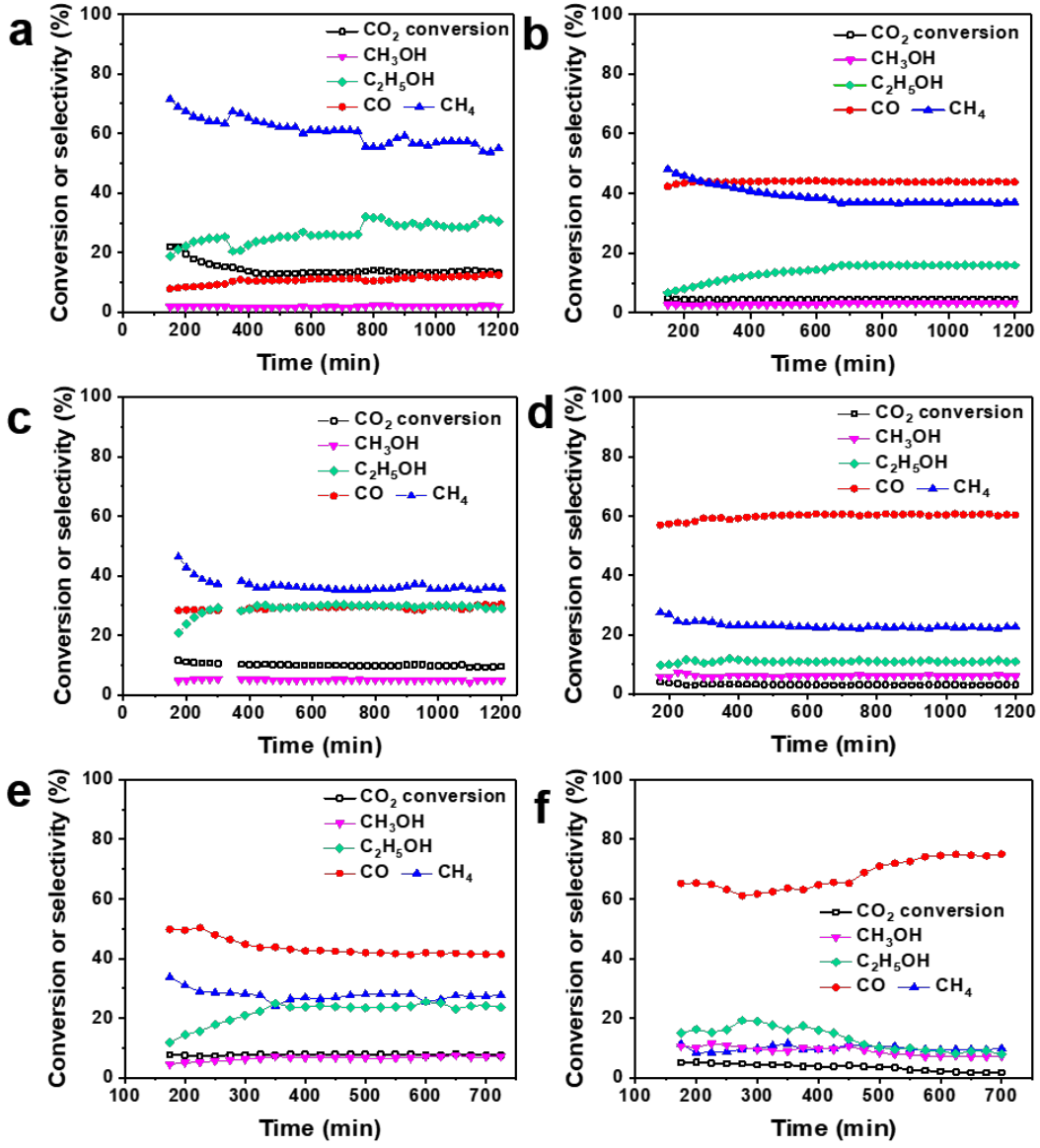

Fig. S7. Stability test and product distribution obtained over 2.5 wt% RhFeLi/TiO_2 NRs (a), 2.5 wt% RhFeLi/TiO_2 Com (b), 2.5 wt% Rh 2.5 wt% FeLi/TiO_2 NRs (c), 2.5 wt% Rh 2.5 wt% FeLi/TiO_2 Com (d), 2.5 wt% Rh 5 wt% FeLi/TiO_2 NRs (e), 2.5 wt% Rh 5 wt% FeLi/TiO_2 Com (f). The molar ratio of Rh:Li is 1:1. Reaction conditions: P = 30 atm, T = 250℃, GHSV = 6000 h^{-1}, $CO_2/H_2/N_2$ = 1/3/1.

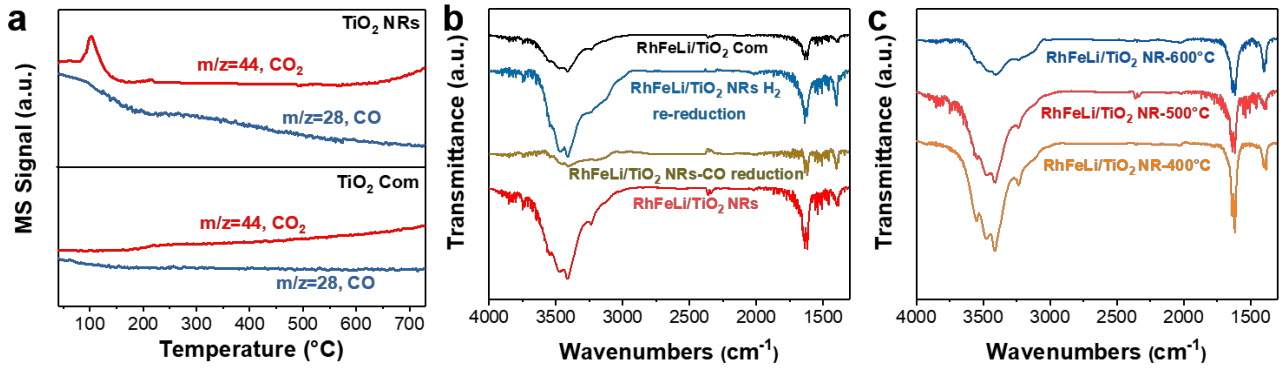

Fig. S8. (a) CO-TPD of pure TiO_2 support: TiO_2 NRs, TiO_2 Com. Pretreatment: H_2 reduction at 400℃ for 1h. (b) FTIR spectra spectra of 2.5 wt% RhFeLi supported on TiO_2 NRs, TiO_2 Com, TiO_2 NRs-CO and TiO_2 NRs-H_2 re-reduction after reaction. (c) FTIR spectra of 2.5 wt% RhFeLi supported on TiO_2 NRs-400℃, TiO_2 NRs-500℃ and TiO_2 NRs-600℃ after reaction.

Note: The hydroxyls over the surface of TiO_2 were charaterized by CO-TPD and FTIR. The peak areas of hydroxyls showed in Fig. 4a and Fig. 6 are obtained from Fig. S8b, c. We integrated peak area of associative -OH stretching vibrations (3450 cm^{-1}) to represent the amount of hydroxyls.

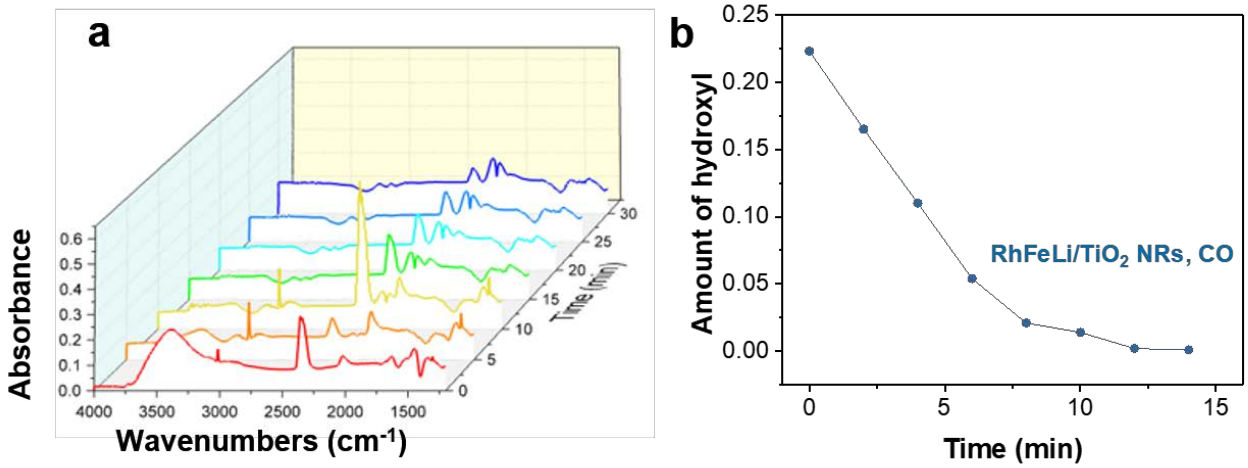

Fig. S9. (a) DRIFTS of CO reduction at 350℃ versus time on the 2.5 wt% RhFeLi/TiO_2 NRs. (b) The amount of -OH at 3450 cm^{-1} in DRIFTS spectra of 2.5 wt% RhFeLi/TiO_2 NRs versus time after feeding CO flow into *in situ* cell at 350℃.

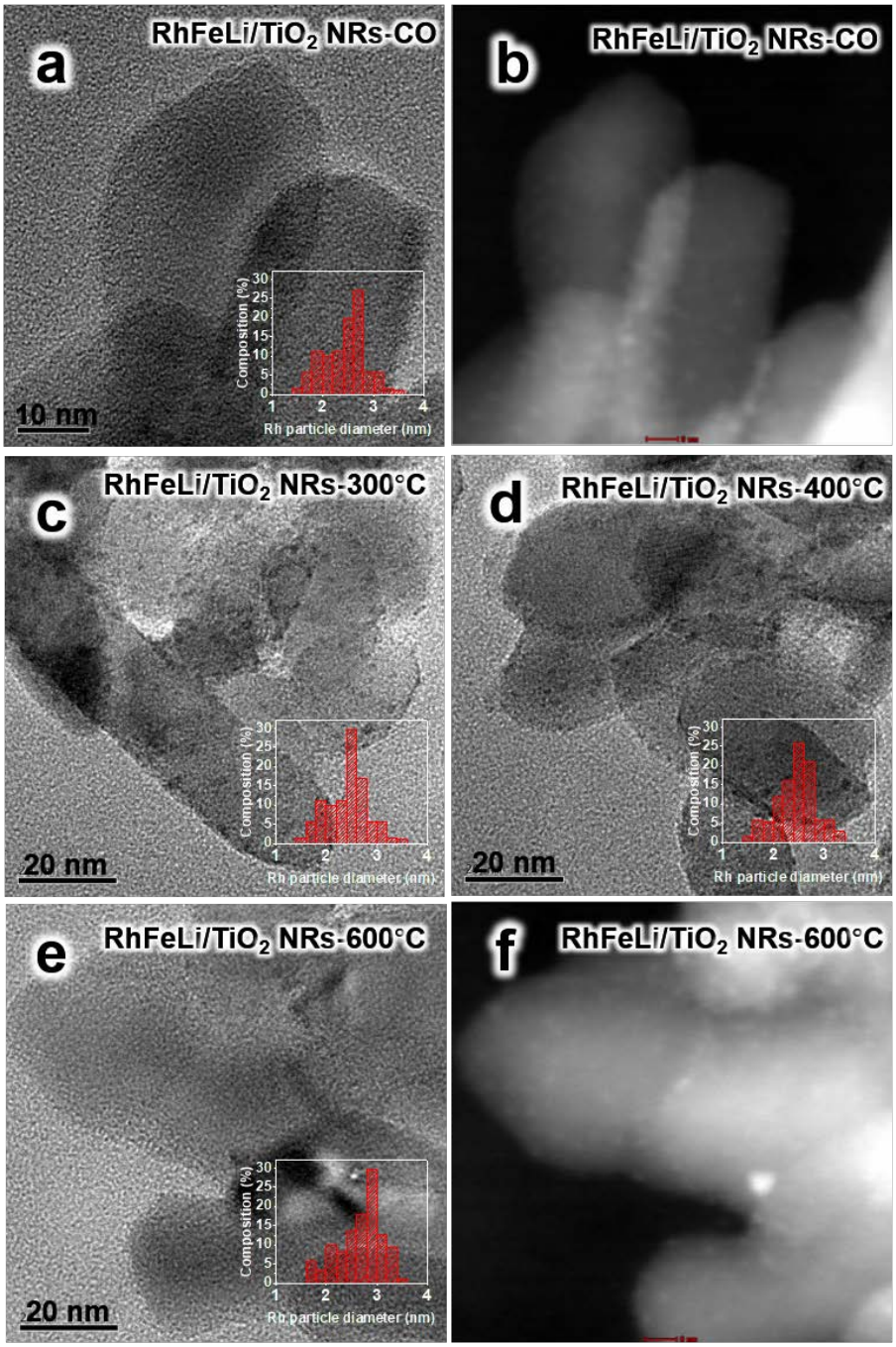

Fig. S10. (a) HRTEM, particle size distributions (Inset figures) and (b) HAADF-STEM images of 2.5 wt% RhFeLi/TiO_2 NRs after CO reduction. (c, d, e) HRTEM, particle size distributions (Inset figures) of 2.5 wt% RhFeLi/TiO_2 NRs-300 ℃, RhFeLi/TiO_2 NRs-400 ℃ and RhFeLi/TiO_2 NRs-600 ℃ after H_2 reduction. (f) HAADF-STEM images of 2.5 wt% RhFeLi/TiO_2 NRs-600 ℃ after H_2 reduction.

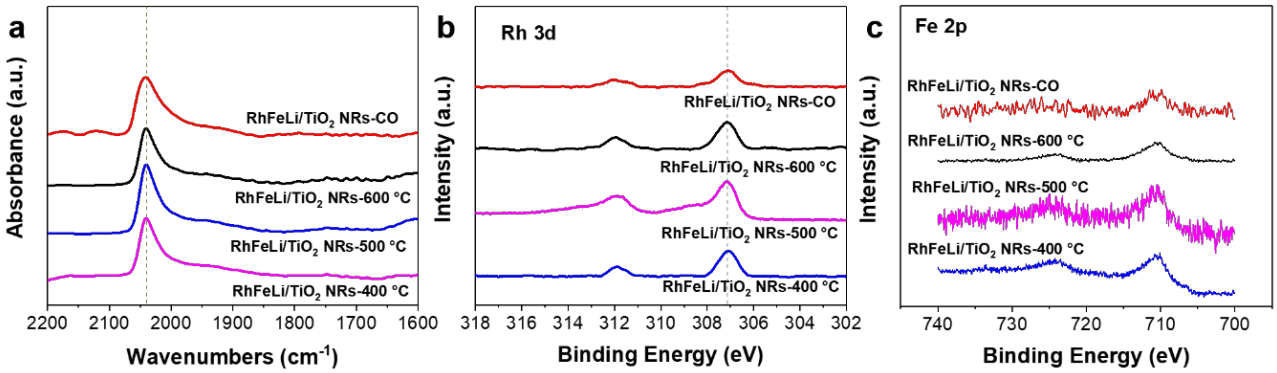

Fig. S11. (a) DRIFTS spectra over 2.5 wt% RhFeLi supported on TiO_2 NRs-CO, TiO_2 NRs-400℃, TiO_2 NRs-500℃ and TiO_2 NRs-600℃ after CO adsorption at 250℃. (b) XPS spectra of Rh 3d obtained from 2.5 wt% RhFeLi supported on TiO_2 NRs-CO, TiO_2 NRs-400℃, TiO_2 NRs-500℃ and TiO_2 NRs-600℃. (c) XPS spectra of Fe 2p obtained from 2.5 wt% RhFeLi supported on TiO_2 NRs-CO, TiO_2 NRs-400℃, TiO_2 NRs-500℃ and TiO_2 NRs-600℃.

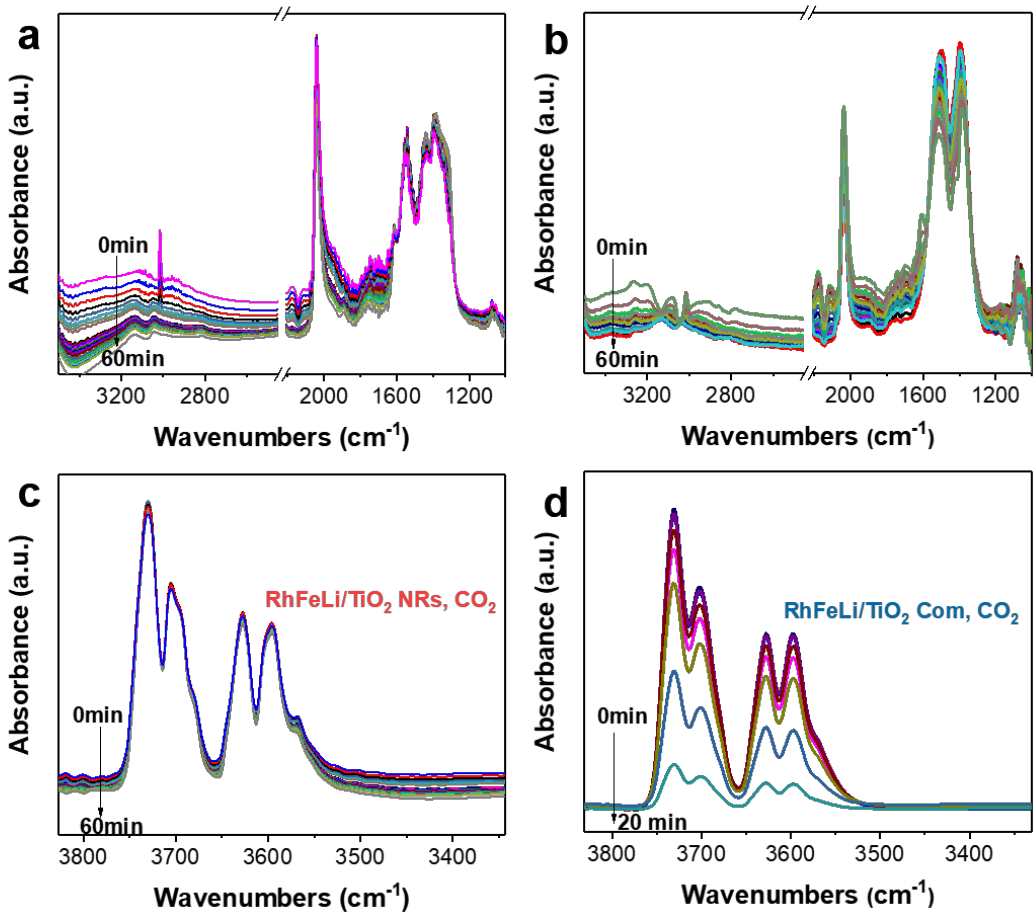

Fig. S12. *In situ* DRIFTS spectra over 2.5 wt% RhFeLi/TiO_2 NRs (a, c) and 2.5 wt% RhFeLi/TiO_2 Com (b, d) after switching the CO_2+H_2+Ar (CO_2:H_2=1:3) flow to pure CO_2 flow at 250 ℃.

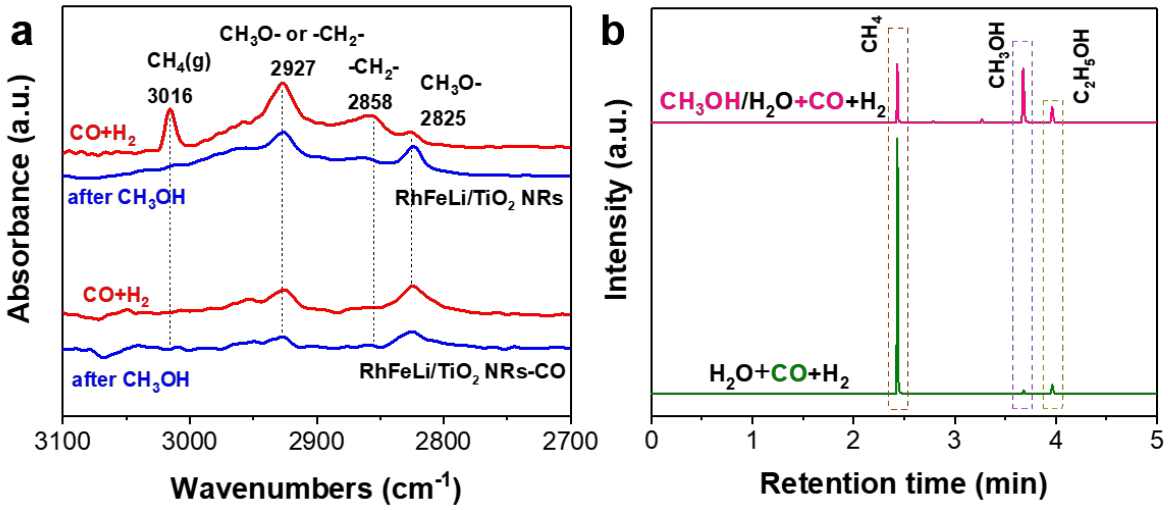

Fig. S13. (a) *In situ* DRIFTS spectra over 2.5 wt% RhFeLi/TiO_2 NRs and 2.5 wt% RhFeLi/TiO_2 NRs-CO after CH_3OH+Ar adsorption followed by CO+H_2 adsorption at 250℃. (b) The GC-FID spectra of gaseous and liquid products produced over 2.5 wt% RhFeLi/TiO_2 NRs with different reactants. Reaction conditions: P = 30 atm, T = 250℃, CO/H_2 = 1/2, the feeding rate of H_2O or CH_3OH/H_2O (CH_3OH/H_2O = 1/10) is 0.5 mL/min.

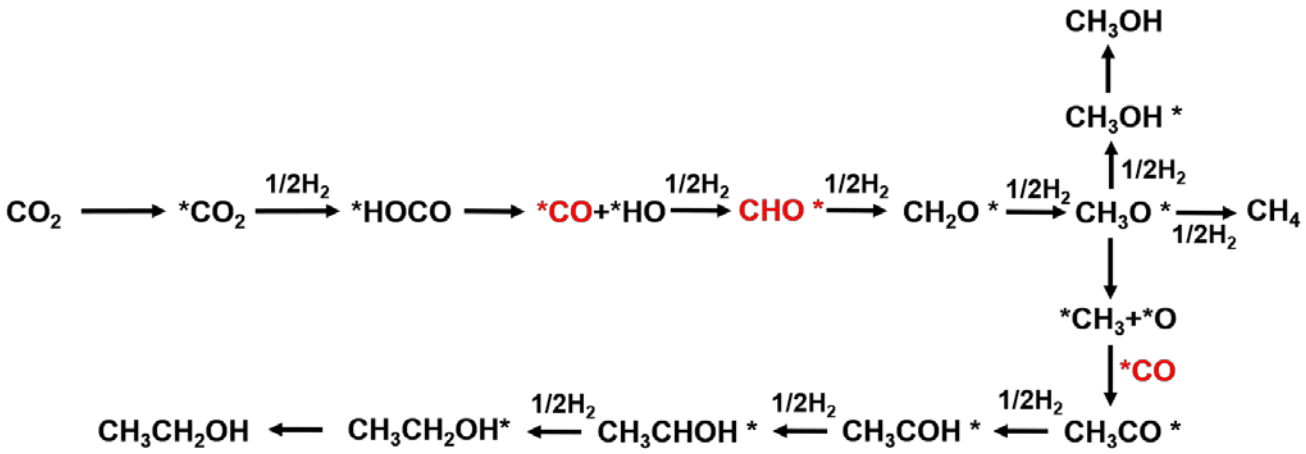

Scheme S1. Conceivable reaction mechanism of CO_2 hydrogenation to ethanol on Rh-based catalyst.

References

1. Y. Wang, H. Luo, D. Liang and X. Bao, *J. Catal.,* 2000, **196**, 46-55.
2. H. Kusama, K. Okabe, K. Sayama and H. Arakawa, *Energy,* 1997, **22**, 343-348.
3. T. Inui and T. Yamamoto, *Catal. Today,* 1998, **45**, 209-214.
4. H. Kusama, K. Okabe, K. Sayama and H. Arakawa, *Catal. Today,* 1996, **28**, 261-266.
5. J. Yang, H. Liu, W. N. Martens and R. L. Frost, *J. Phy. Chem.C,* 2010, **114**, 111-119.
6. V. P. Santos, O. S. G. P. Soares, J. J. W. Bakker, M. F. R. Pereira, J. J. Órfão, M.; J. Gascon, F. Kapteijn and J. L. Figueiredo, *J. Catal.,* 2012, **293**, 165-174.